Science of the Total Environment 666 (2019) 559–571

Contents lists available at ScienceDirect

Science of the Total Environment

journal homepage: www.elsevier.com/locate/scitotenv

Human health risk assessment for the occurrence of enteric viruses in drinking water from wells: Role of flood runoff injections

Costantino Masciopinto [a,*], Osvalda De Giglio [b], Maria Scrascia [c], Francesca Fortunato [d], Giuseppina La Rosa [e], Elisabetta Suffredini [f], Carlo Pazzani [c], Rosa Prato [d], Maria Teresa Montagna [b]

[a] Consiglio Nazionale delle Ricerche, Istituto di Ricerca Sulle Acque (IRSA), Reparto di Chimica e Tecnologia delle Acque, Bari, Italy
[b] Dipartimento di Scienze Biomediche e Oncologia Umana, Università degli Studi Aldo Moro, Bari, Italy
[c] Dipartimento di Biologia, Università degli Studi Aldo Moro, Bari, Italy
[d] Dipartimento di Scienze Mediche e Chirurgiche, Università di Foggia, Italy
[e] Dipartimento Ambiente e Salute, Istituto Superiore di Sanità, Roma, Italy
[f] Dipartimento di Sicurezza Alimentare, Nutrizione e Sanità Pubblica Veterinaria, Istituto Superiore di Sanità, Roma, Italy

HIGHLIGHTS

- Human health impact of prolonged floodwater injections in groundwater
- Climate change impact makes virus presence in carbonate aquifers more likely.
- Floodwater can enable virus detachments from *terra rossa* in limestone aquifers.
- Virus occurrence in drinking water from wells far 8 km from flooding injections
- Low count of fecal indicators does not prevent virus occurrence in drinking water.

GRAPHICAL ABSTRACT

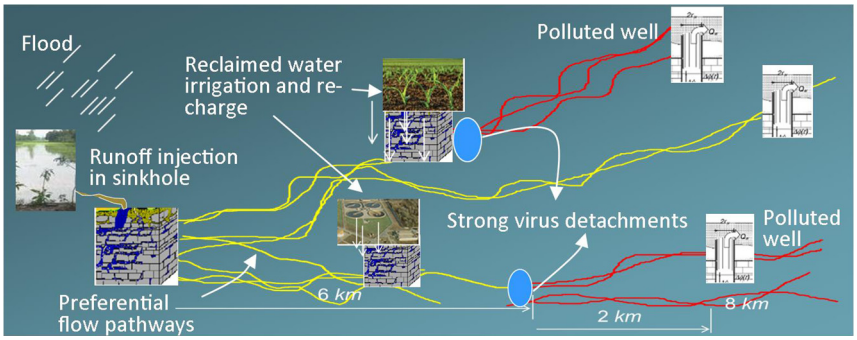

ARTICLE INFO

Article history:
Received 8 October 2018
Received in revised form 6 February 2019
Accepted 7 February 2019
Available online 10 February 2019

Editor: Damia Barcelo

Keywords:
Groundwater drinking water quality
Flood impact
Virus transport model
Infection dose-response model
Health-risk impact

ABSTRACT

We demonstrated that floods can induce severe microbiological contamination of drinking water from wells and suggest strategies to better address water safety plans for groundwater drinking supplies. Since 2002, the Italian Water Research Institute (IRSA) has detected hepatitis A virus, adenovirus, rotavirus, norovirus, and enterovirus in water samples from wells in the Salento peninsula, southern Italy. Perturbations in the ionic strength in water flow can initiate strong virus detachments from *terra rossa* sediments in karst fractures. This study therefore explored the potential health impacts of prolonged runoff injections in Salento groundwater caused by severe flooding during October 2018. A mathematical model for virus fate and transport in fractures was applied to determine the impact of floodwater injection on groundwater quality by incorporating mechanisms that affect virus attachment/detachment and survival in flowing water at microscale. This model predicted target concentrations of enteric viruses that can occur unexpectedly in wells at considerable distances (5–8 km) from the runoff injection site (sinkhole). Subsequently, the health impact of viruses in drinking water supplied from contaminated wells was estimated during the summer on the Salento coast. Specific unpublished dose-response model coefficients were proposed to determine the infection probabilities for Echo-11 and Polio 1 enteroviruses through ingestion. The median (50%) risk of infection was estimated at $6.3 \cdot 10^{-3}$ with an uncertainty of 23%. The predicted burden of diseases was 4.89 disability adjusted life years per year, i.e., twice the maximum

Abbreviations: AdV, adenovirus; EV, enterovirus; HAV, hepatitis A virus; HEV, hepatitis E virus; NoV, norovirus; PV, poliovirus; RoV, rotavirus; IP, infective particles; DALY, disability adjusted life year; IS, ionic strength; MID, minimum infectious dose.

* Corresponding author.
E-mail address: costantino.masciopinto@ba.irsa.cnr.it (C. Masciopinto).

https://doi.org/10.1016/j.scitotenv.2019.02.107

tolerable disease burden. The results highlight the requirement for additional water disinfection treatments in Salento prior to the distribution of drinking water. Moreover, monthly controls of enteric virus occurrence in water from wells should be imposed by a new water framework directive in semiarid regions because of the vulnerability of karst carbonate aquifers to prolonged floodwater injections and enteric virus contamination.

1. Introduction

In semiarid regions, such as Salento, Italy, rainfall runoff and treated secondary municipal effluents are collected by stream channels and used to recharge groundwater by sinkholes (Masciopinto et al., 2008). Treated municipal effluents are either spread on the soil or transferred in ditches or artificial ponds (or basins) to recharge groundwater (Keswick and Gerba, 1980). The simple chlorination treatment used to disinfect such effluent has been shown to be inadequate for the complete removal of viruses from water (Costán-Longares et al., 2018; Peyment and Franco, 1993). In addition, wastewater leakage and overflow from septic tanks in tourist villages, farms, and private houses can further contribute to virus and nutrient accumulation in subsoil and groundwater. Furthermore the current flooding height during October in Salento has tripled since 1923 due to the increased impact of climate change, as shown by precipitation intensities recorded by the *Protezione Civile* (Supermeteo, 2018) at the Galatina station. Floodwater may contain intestinal bacteria and viruses that cause severe diseases 10–30 days after water direct ingestion, contact, or inhalation (Paterson et al., 2018), but the time of flooding removal via runoff injections in sinkholes may require >20 days.

Although wastewater soil/subsoil filtration has long been known as an effective process for eliminating pathogens from wastewater (Schoenen, 2002), soil aquifer treatment and successive water chlorination cannot be considered an appropriate disinfection barrier for drinking water (Ayuso-Gabella et al., 2011). The effective disinfection of water cannot be uniformly ensured without a proper disinfection treatment train (Pecson et al., 2017), and the microbial contamination of wells that supply drinking water could lead to water-associated disease outbreaks.

In the Salento peninsula, concerns arose in 1997 regarding groundwater quality supplied after simple chlorination due to an abrupt increase in the incidence of hepatitis A cases during that year (Masciopinto et al., 2007), which was approximately five times higher than the typical national yearly value (2–3 per 100,000 inhabitants). The hepatitis A and gastrointestinal outbreaks were mainly attributable to the ingestion of contaminated food and water from wells polluted by wastewater injections. Thus, the government started innovating and rebuilding many municipal treatment plants by including tertiary treatment plants at recharge sites where indirect surface methods (i.e., ditches, ponds, and soil spreading) and water reuse for irrigation have replaced previous injection wells. The annual incidence of HAV infections after 2006 was reduced to a minimum in Salento (1–2 cases per year), also as a result of the vaccination program (Lopalco et al., 2008), but recorded cases in the Puglia region (MalInf, 2017, 2018) (Fig. 1) suggest that in recent years several HAV infections could have originated from contaminated drinking water.

Groundwater monitoring results (Table 1) have further revealed the occurrence of numerous enteric viruses, e.g., adenovirus (AdV), enterovirus (EV), such as poliovirus (PV) and echoviruses, hepatitis A virus (HAV), *Norovirus* genotypes I (GI) and II (GII), protozoans (*Giardia* and *Cryptosporidium* spp.), and pathogenic bacteria in the regional karstic fractured aquifers of Murgia and Salento. Harmful illnesses related to viral infections that may lead to chronic disabilities and mortality are reported in the same table. Lugoli et al. (2011) suggested that the Salento population is currently exposed to a high risk of water-related diseases, such as typhoid fever, via fecal pathogen transmission.

The present study focused on the indirect and delayed health impact, which is caused by intensive floodwater injections in groundwater by sinkholes. In particular, we estimated current water-related gastroenteric diseases that may occur in Salento by considering the ingestion of contaminated water derived from wells. The delay of diseases with respect to the time of a flood event is mainly attributable to the length of time required (i.e., up to two years) for the injected floodwater to be transported through the subsoil before reaching the contaminated target wells. This means that prolonged injections of floodwater into a sinkhole (i.e., >20–30 days) can produce chemical perturbations in water flowing through fractures, enabling the unexpected strong releases of previously attached viruses and indirect contamination of drinking water, even in wells as far as 5–8 km from the sinkhole (Masciopinto et al., 2008).

The mathematical model used to simulate virus fate and transport in this study incorporated the effects of attachment/detachment/

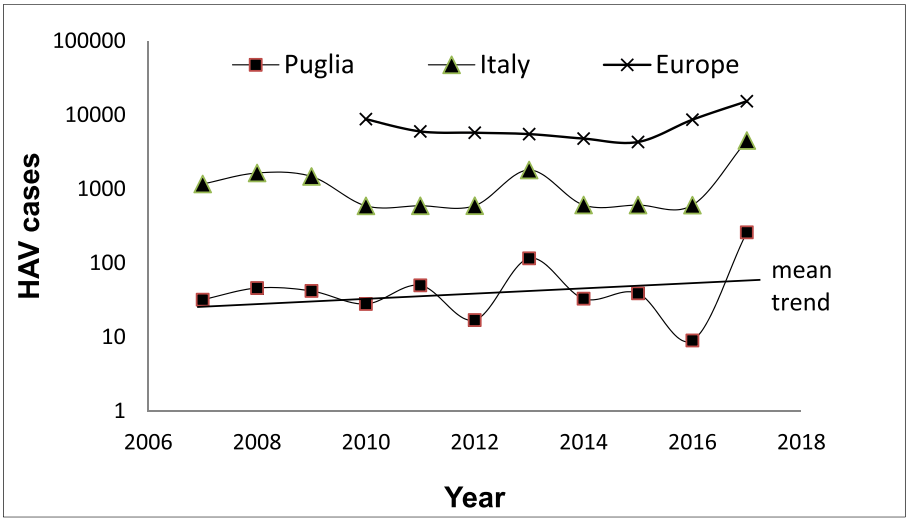

Fig. 1. Comparison of notified (i.e., confirmed) hepatitis A cases in Europe (ECDC, 2018), Italy (SEIEVA, 2017), and the Puglia region (MalInf, 2018) from 2007 to 2017.

Table 1
Enteric viruses detected in wells in Salento/Murgia aquifers near artificial recharge sites in 2002–2005 (Masciopinto et al., 2007; Masciopinto et al., 2011), 2014 (Masciopinto et al., 2017), and 2016–2017 (De Giglio et al., 2016, 2017).

	Sampling date:	2002–2005	2014	2016–2017
Pathogenic agent	Illnesses associated (Craun and Calderon, 1997)	Salento	Salento/Murgia	***This work*** Salento
ADV	Gastroenteritis	Positive		
HAV	Hepatitis	0	0	Positive to HAV IB
NoV	Gastroenteritis	20 gc/l GI and 1000 gc/l of GII	Positive	Positive to GII.4
RoV	Gastroenteritis		Positive	Positive
EV			$5.07 \cdot 10^4$ gc/l	Positive
Echovirus (ECHO-11)	Gastroenteritis	12.5 gc[a]/l		
PV[c]	Gastroenteritis, meningitis, paralysis, myocarditis and heart diseases, rash, fever, encephalitis, pleurodynia, eye infections and diabetes mellitus	From $10^{-5.5}$ $CCID_{50}$[b]/25 μl to 10^{-4} $CCID_{50}$/25 μl		

[a] gc stands for gene copies.
[b] CCID50 stands for virus infectious units in a suspension volume that infect 50% of a cell cultured in petri dishes or tubes.
[c] Poliovirus data refer to 2002, the year during which the vaccination program switched to the IPV-only schedule, thus dramatically reducing the quantity of PV excreted into the environment.

inactivation at microscale can affect the concentrations of suspended viruses in water flowing through fractures. The modeled target concentration at one of these wells was then used to determine the infectious dose ingested and the corresponding probability level of infection and health risk to residents and tourists of the Salento coastal area during summer. The risk impact was initially calibrated on the basis of the notified cases of hepatitis A throughout Salento. This calibration permitted the assessment of primary and secondary morbidity coefficients. The current summer illness risk for residents and tourists due to simultaneous ingestion of AdV, NoV, HAV, rotavirus (RoV), and EV in drinking water could then be estimated. The risk impact, i.e., the disease burden, was quantified in terms of disability adjusted life years (DALYs).

2. Study area: Salento peninsula

The semiarid region of the Salento peninsula does not have surface water, and over 70% of required drinking water is derived from groundwater. Groundwater discharge is expected to decline in the future due to the impacts (e.g., sea level rise) of climate change (Masciopinto and Liso, 2016). Groundwater in Salento flows under pressure through fractures in the limestone rock formations (Cotecchia, 1977), known as Calcare di Melissano (Turonian-Santonian) and Calcare di Altamura, i.e., carbonate bedrocks. The thickness of saturated aquifers ranges from 60 m inland to 10 m closer to the coast, and about 10 km inland they are overlain by sandstone and calcareous deposits of 60–70 m thick. The limestone formations are locally interposed by lenses of *terra rossa* and are overlain by Tertiary (Miocene) sandstone deposits (Pietra Leccese and Calcareniti di Andrano). More recent deposits include the Open Shelfs (Pliocene), Subappinnine clays (Lower Pleistocene), calcareous breccia, sands (Sabbie di Uggiano la Chiesa, Middle-Upper Pliocene), and *terra rossa*. The Salento aquifer is very permeable throughout because it contains a great number of joints and fractures caused by tectonic movements that have been karstified and locally filled with *terra rossa* deposits.

Terra rossa (Merino and Banerjee, 2008) is formed by calcite minerals being replaced with authigenic clay containing Fe, Al, and Si oxides precipitated from dissolved ions during the karstification process of carbonate rocks. The mineral composition of *terra rossa* may include 45% silica (quartz, feldspar, and calcite), 25% aluminum oxides (kaolinite), 15% iron oxides (hematite, magnetite, and goethite)—which give the soil its red color—and trace amounts of calcium, potassium, titanium, magnesium, sodium, manganese, and phosphorus oxides (Masciopinto and Visino, 2017).

Numerous (~25) sinkholes and caves in the study area directly connect the surface water and groundwater. The effective porosity of fractures was estimated to be 0.005 ± 0.002 p.u. via pumping well tests (Masciopinto et al., 2008), and water infiltration rate measurements in vertical fractures via large ring infiltrometers provided values higher than 8.2 m/day under field saturated conditions (Masciopinto and Caputo, 2011). The average ground elevation in the studied area is approximately 90 m above sea level, and water depth in wells is 87–89 m below ground level. At a distance of 20 km from the coast, the pressure head gradient lies 3 m above sea level.

3. Sampling and virus detection methods

The Puglia government (Progetto Maggiore, 2015) performs two seasonal samplings per year from about 300 wells across the Salento and Murgia regions as part of a survey program. We selected 20 such wells in 2016–2017 to determine the occurrence of enteric viruses in the Salento groundwater (Fig. 2).

Fig. 2 shows anthropogenic activities and land use in the study area that could have impacted the groundwater quality observed in wells I1147 and I1126. In the study area, there is not much intensive cultivation, with only olive production being relevant (over 60% of the area). Grains, fruits, and vegetables (e.g., watermelon and tomato) are cultivated in small scattered areas that cover <5% of the study area. The remainder of the area (35%) is urbanized or uncultivated with many towns, industries, and caves.

From each well, 20 *l* of pumped water was collected in sterile vessels and transported under refrigeration (+4 °C) to the Bari University Laboratory for pre-filtration and successive virus and bacteria assays. Enteric virus detection was performed using nested polymerase chain reaction (PCR) followed by sequencing and quantitative (gene copies) real-time PCR. Fecal indicators (Table 2) were detected using standard Environmental Protection Agency methods (www.epa.gov/water-research/microbiological-methods-and-online-publications). The results showed very low concentrations of total bacterial count (TBC), total coliforms and *Escherichia coli*, as well as of nitrates in monitored wells, although some traces of ammonia and *E. coli* at 21 cfu/100 ml were observed in water sampled during April 2017 from wells I1190 and I1147 (see Table 2), respectively.

3.1. Sample concentration and viral RNA purification

The rapid concentration method D of Schultz et al. (2011) and, the ISO 15216-1 (2017) and ISO/TS 15216-2 (2013) methods were followed in this study. Each water sample (20) was filtered through a 47 mm (diameter) electropositive charged membrane with a pore size of 0.45 μm (Millipore, Burlington, MA, USA) by means of a vacuum pump. Each filtrated sample was then concentrated via tangential flow ultrafiltration (Vivaflow 200, Vivascience Ltd, UK) using membranes (www.sartorius.com) previously conditioned with beef extract (at *p*H 7) to minimize virus adsorption onto the filter membranes.

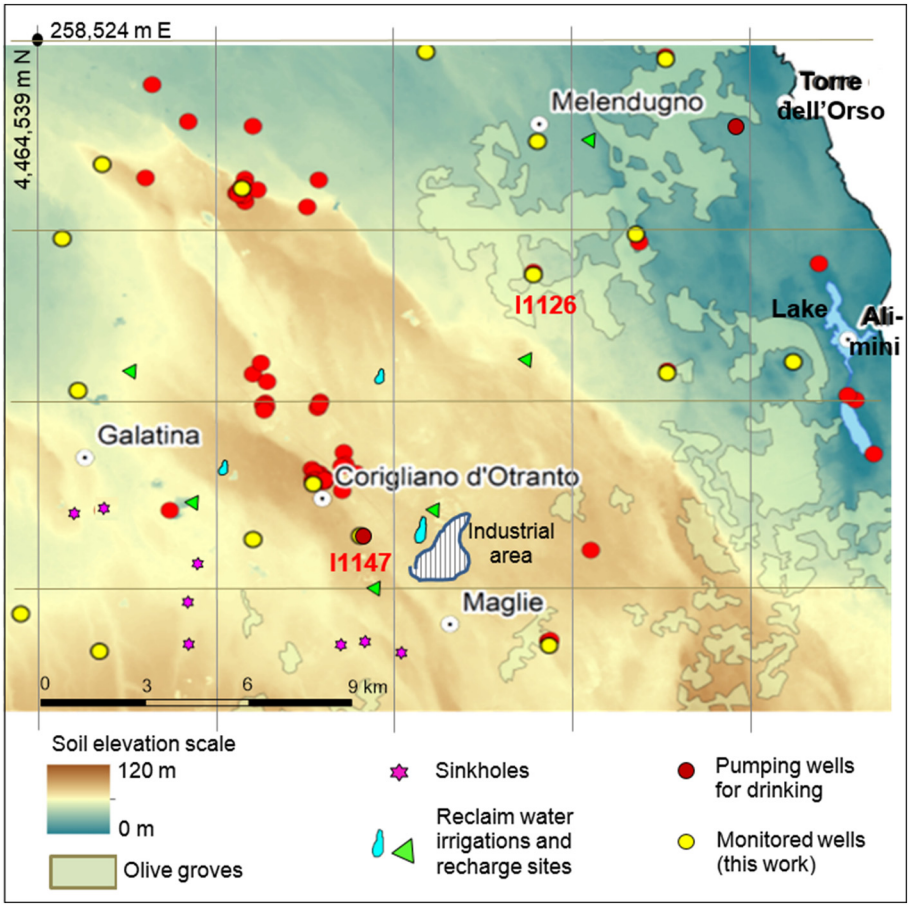

Fig. 2. Anthropogenic activities and land use (olive groves, towns, industrial area, sinkholes, reclaimed water irrigation and recharge sites) in the study area that could have impacted the groundwater quality observed in wells I1147 and I1126, as well as positions of wells for drinking water supply and groundwater monitoring.

Table 2
Chemical and microbiological water quality before chlorination of drinking water from three Salento wells that resulted contaminated by enteric viruses.

ID well	I1126	I1147	I1190	I1126	I1147	I1190	Flood runoff
Sampling date	Nov 2016			April 2017			Average values
Chemical parameters (mg/l)							
Specific cond. (μS/cm)	568	532	1211	822	697	1607	600
Temperature °C	14.1	14.3	15.3	14.5	14.1	15.8	12
pH	7.37	7.22	7.28	7.37	7.22	7.28	7.1
NH_4^+	<0.05	<0.05	0.09	<0.05	<0.05	0.09	0.2
NO_3^-	23	21	49	23	21	49	1.2
Br^-	<1	<1	<1	<1	<1	<1	–
Cl^-	61	26	240	161	130	253	13
F^-	0.17	0.23	0.17	0.17	0.23	0.17	–
PO_4^{3-}	<1	<1	<1	<1	<1	<1	0.41
NO_2^-	<0.1	<0.1	<0.1	<0.1	<0.1	<0.1	<0.05
SO_4^{2-}	13	10	50	43	35	50	9
Ca^{2+}	72	76	103	110	95	123	100
Mg^{2+}	16	30	40	47	41	65	5
K^+	2	2	4	6	8	10	1.2
Na^+	35	19	130	120	93	251	10
Total alkalinity as HCO_3^-	310	250	390	410	312	480	138
Estimated IS (mM)	7.8	7.6	16.8	16.1	13.2	23.0	5.3
Microbiological parameters							
Total *coliforms* cfu/100 ml	0	50	0	0	60	0	9180
E. coli cfu/100 ml	0	0	0	0	21	0	4
Enterococci cfu/100 ml	0	0	0	0	0	0	210
Total bacterial count cfu/ml							
37 °C	0	150	0	3	70	140	13,400
22 °C	0	30	0	5	40	220	10,300
Enteric viruses occurrence/count	Not detected	Not detected	Not detected	Positive EV	Norovirus GII.4 4.48 ± 1 gc/l	Positive Hepatitis A IB	20.6 cfu/ml somatic coliphages

Following this first ultrafiltration step, each concentrated sample (300 ml) was loaded with elution products of both the polyether sulfone 10,000 Da and electropositive membranes by using 3% beef extract at *p*H 9.5, namely Tris glycine beef extract (Tris, 12 g/l; glycine, 3.8 g/l; and beef extract, 10 g/l). Each sample was poured into a sterile tube and buffered using HCl solution at 0.1 N. Each tube was transferred to an ultracentrifugal filter unit (Amicon Ultra-2, Ultracell-10 membrane, Millipore) with 15 ml capacity at 4000 ×*g* for 15 ± 1 min using a 10 kDa MWCO membrane. Each re-concentrated sample (100–400 μl) was then poured into a sterile tube, and the volume size was increased to 500 μl by adding PBS (NaCl, 8 g/l; KCl, 0.2 g/l; Na_2HPO_4, 1.15 g/l; and KH_2PO_4, 0.2 g/l in distilled water) and buffered. Ribonucleic acid (RNA) extraction was then performed using the ZYMO Direct-zol™ RNA MiniPrep device (Zymo Research, Irvine, CA, USA). The RNA extracted from each sample was diluted with 60–80 μl of DNase/RNase-free water and frozen at −80 °C.

3.2. Nested reverse transcription-PCR

NoV GI and GII, EV, HAV, hepatitis E virus, and AdV were tested using nested reverse transcription (RT)-PCR with the primers shown in Table 3. RNA (2 μL) and 10 pmol of forward and reverse primers were used in the first PCR, in a final mixture of 25 μL, using the MyTaq One Step RT-PCR kit (Bioline Ltd, London, UK), which was formulated for highly reproducible first-strand cDNA synthesis and subsequent PCR in a single tube. Amplification conditions were as follows: RT at 42 °C for 30 min, followed by RT at 95 °C for 2 min, 35 amplification cycles of denaturation for 30 s at 95 °C, annealing for 30 s (51 °C for HEV, 42 °C for EV, 50 °C for NoV, and 58 °C for HAV), and extension at 72 °C for 1 min. Final incubation was performed at 72 °C for 10 min.

Nested PCR was then performed with the MyTaq Red Mix (Bioline Ltd, London, UK), using 1 μl of the PCR product from the first step as a template. The nested PCR reaction conditions were 95 °C for 2 min, followed by 35 amplification cycles of 30 s at 95 °C, annealing for 30 s at the various annealing temperatures (48 °C for HEV, 60 °C for EV, 50 °C for NoV, and 50 °C for HAV), and extension at 72 °C for 1 min. A final incubation step was performed at 72 °C for 10 min. For AdV, the MyTaq Red Mix kit was used for both the first and nested cycles. Positive and negative controls were systematically used, and standard precautions were taken to prevent cross-contamination. Positive PCR products were purified using Montage PCRm96 Micro-Well Filter Plates (Millipore, Burlington (MA), US) and sequenced in both strands (Bio-Fab Research, Rome, Italy). Consensus sequences were reconstructed using Molecular Evolutionary Genetics Analysis software, version 7.0, and the relatedness of the sequences were evaluated using the National Center for Biotechnology Information's Basic Local Alignment Search Tool (BLAST; http://blast.ncbi.nlm.nih.gov/Blast.cgi).

3.3. Real-time quantitative RT-PCR

Quantification was performed via real-time quantitative RT-PCR (RT-qPCR) for samples that showed positivity after analysis via qualitative nested PCR. The assay described by Donaldson et al. (2002) was used for EV with a standard curve of synthetic RNA as explained by La Rosa et al. (2010). The real-time RT-qPCR standard method described by ISO 15216-1 (2017) was applied for HAV and NoV GII. The reagents and conditions applied for ISO 15216-1 were those reported in the annexes of the standard method. Results are shown in Table 2, and all primers and probes used are described in Table 3. Each sample was

Table 3
Primer and PCR applied in this study.

Virus	Primer	Sequence 5′-3′	PCR cycle	PCR product (bp)	Reference
Norovirus GI	COG1F	CGY TGG ATG CGN TTY CAT GA	First	381	Kojima et al., 2002; Kageyama et al., 2003
	G1-SKR	CCAACCCARCCATTRTACA			
	G1-SKF	CTG CCC GAA TTY GTA AAT GA	Nested	330	
	G1-SKR	CCA ACC CAR CCA TTR TAC A			
Norovirus GII	COG2F	CAR GAR BCN ATG TTY AGR TGG ATG AG	First	387	
	G2-SKR	CCRCCNGCATRHCCRTTR TAC AT			
	G2-SKF	CNTGGGAGGGCGATCGCAA	Nested	344	
	G2-SKR	CCRCCNGCATRHCCRTTRTACAT			
Norovirus GII	QNIF2	ATGTTCAGRTGGATGAGRTTCTCWGA	Real-time RT-(q)PCR	–	Loisy et al., 2005; Kageyama et al., 2003
	COG2R	TCGACGCCATCTTCATTCACA			
	QNIFs	FAM-AGCACGTGGGAGGGCGATCG-TAMRA			
Hepatitis A	1852	TATTCAGATTGCAAATTAYAAT	First	393	La Rosa et al., 2014
	1853	AAYTTCATYATTTCATGCTCCT			
	1854	TATTTGTCTGTYACAGAACAATCAG	Nested	267	
	1855	AGGRGGTGGAAGYACTTCATTTGA			
	HAV68	TCACCGCCGTTTGCCTAGGGAGAG	Real-time RT-(q)PCR	–	Costafreda et al., 2006
	HAV240	CCCTGGAAGAAAGCCTGAACCT			
	HAV150-	FAM-GCAGGAATTAA-MGBNFQ			
Hepatitis E	ORF1F	CCAYCAGTTYATHAAGGCTCC	First	348	Fogeda et al., 2009
	ORF1R	TACCAVCGCTGRACRTC			
	ORF1FN	CTCCTGGCRTYACWACTGC	Nested	172	
	ORF1RN	GGRTGRTTCCAIARVACYTC			
Enterovirus	Ent1	CGGTACCTTTGTACGCCTGT	First	545	Pina et al., 1998
	Ent2	ATTGTCACCATAAGCAGCCA			
	neEnt1	TCCGGCCCCTGAATGCGGCTA	Nested	123	
	neEnt2	GAAACACGGACACCCAAAGTA			
	EV-U	GGCCCCTGAATGCGGCTAAT	Real-time RT-(q)PCR	–	Donaldson et al., 2002; La Rosa et al., 2010
	EV-D	CACCGGATGGCCAATCCAA			
	EV-Pr	FAM-CGGACACCCAAAGTAGTCGGTTCCG-TAMRA			
Adenovirus	AdhexF1	TICTTTGACATICGIGGIGTICTIGA	First	764–896	Lu and Erdman, 2006
	AdhexR1	CTGTCIACIGCCTGRTTCCACA			
	AdhexF2	GGYCCYAGYTTYAARCCCTAYTC	Nested	688–821	
	AdhexR1	GGTTCTGTCICCCAGAGARTCIAGCA			
Rotavirus	1950	GCAGTYGTTGYTGYHACTTCAACR	First	986	Zeng et al., 2008; La Rosa et al., 2017
	NSP3r	GGTCACATAACGCCCCTATAGC			
	1958	GTCATCAGTTGAGTGGTATCTAAGRT	Seminested	324	
	NSP3r	GGTCACATAACGCCCCTATAGC			

FAM: 6-carboxyfluorescein; TAMRA: 6-carboxytetrameth-ylrhodamine; MGBNFQ: (minor groove binder/non-fluorescent quencher).

assayed in duplicate using 5 μL undiluted nucleic acid extract in a final volume of 25 μL. Two negative controls were included in each assay.

Plasmids containing the PCR target region were used for the construction of the standard curves. The PCR product was the number of base pairs (bp), i.e., the size of the genome segment amplified by PCR. Quantification results were considered acceptable if the determination coefficient R^2 (−) and negative slope of the standard curve were >0.98 and 3.1–3.6, respectively.

4. Risk assessment method

Mathematical models that treat pathogens as colloids are useful for determining pathogen counts in aquifers, making them useful in the evaluation of potential long-term health risks associated with the occurrence of enteric viruses in Salento groundwater (Masciopinto et al., 2008). Model predictions can evaluate virus concentrations and identify infectious doses that might harm the target populations. Model simulations require appropriate input data, such as the position of the primary source of groundwater contamination and hydrogeological and geochemical data. The applied model in this study was previously calibrated (Masciopinto et al., 2011) by using monitoring results of water sampled from wells of the Nardò injection site about 20 km west of well I1147 (see Fig. 2). Validations and calibration of the same model (Masciopinto, 2007) provided an uncertainty of 23% of the final predictions of virus infective particles (IP) in water from the wells. The uncertainty was due to the approximate (±8%) estimation of the total virus reduction rate coefficients and the tolerance (±15%) of the spatial variability estimation of the fracture aperture covariance at the model scale, which is based on the validity of the ergodic hypothesis.

4.1. Groundwater flow

The conceptual model used to simulate water flow in the fractured limestone was layered, i.e., it featured a sequence of identical parallel horizontal fractures in the x–y plane. Each fracture had a variable aperture size in the fracture plane. Generally, at least 30–40 results of pumping well tests were necessary to accurately resolve the fracture-aperture spatial variability of the studied aquifer by means of experimental variograms (Masciopinto, 2005) of the spatial aperture covariance variability. The best fit of the experimental variograms using exponential models was used to transfer the aquifer heterogeneities to the fracture flow solutions.

Each horizontal facture was discretized into x and y directions by using appropriate grid step sizes (large step sizes decrease the precision of the results). The water flowrate in each elementary grid channel was estimated using the following equation (Masciopinto et al., 2008), which was derived from the Darcy–Weisbach flow equation in a conduit:

$$\left(\phi_i - \phi_j\right) = Q_{ij}^{\,2}\left[\frac{f_f}{2g\Delta y}\frac{\Delta x}{\Delta y}\left(\frac{1}{(2b_i)^3}+\frac{1}{(2b_j)^3}\right)\right] \quad (1)$$

where f_f (−) is the friction factor that accounts for non-laminar flow; Q_{ij} (L^3/t) is the local discharge between generic grid nodes *i* and *j*, with piezometric heads ϕ_i and ϕ_j; *g* (L/t^2) is the gravity acceleration; and $2b_i$ is the fracture nodal aperture of the grid with step sizes Δx (240 m) and Δy (240.7 m). The groundwater flow results, i.e., heads and water velocity vectors of the study area (12 × 13 km^2), are shown in Fig. 3 as a 2D representation of the study area obtained by Surfer (v. 11.6.1159; www.goldensoftware.com). The flow model output file (x, y, piezometric head, and water velocity) was elaborated by Surfer to obtain the contour of piezometric head and water velocity vectors in each grid channel of the studied domain. Directions, lengths, and positions of the velocity vectors were according to the calculations made by the applied groundwater flow model. The flow velocity in the fractures ranged from 1 to 50 m/day with an average value of 12 m/day. This output was used as input for the virus transport model.

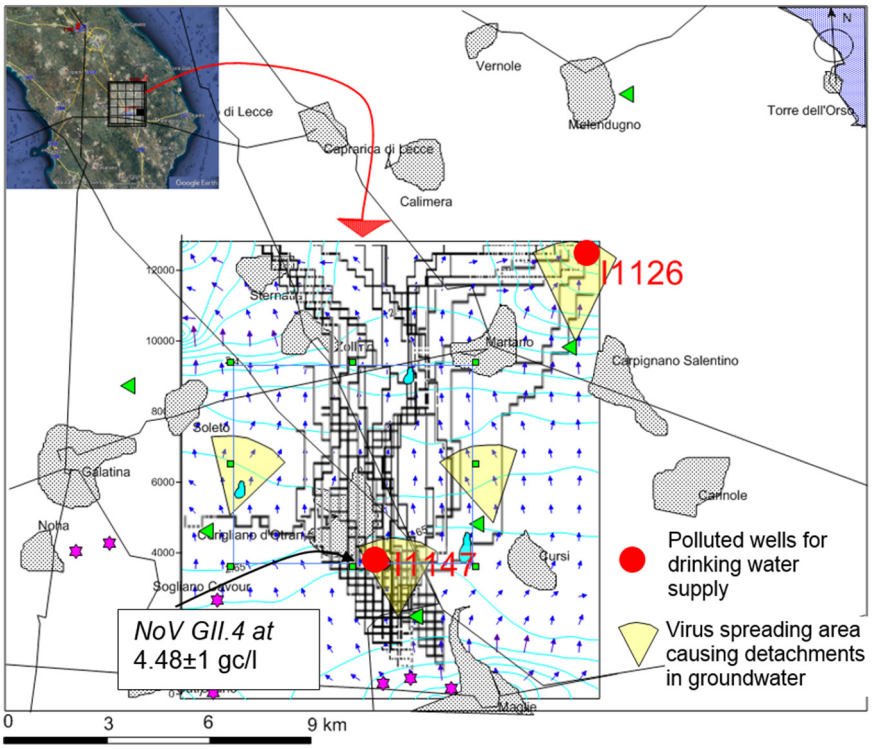

Fig. 3. Flow and transport model solutions in Salento groundwater: Flow velocity vectors (average of 12 m/day) and virus runoff pathways (black lines and squares) after injection into sinkholes (violet stars) near Maglie.

4.2. Runoff and pathogen transport pathways: particle tracking

The particle tracking technique was applied to determine the preferential pathways through the aquifer followed by viruses in injected wastewater (runoff) and, of viruses subsequently detached from the *terra rossa* in flowing water in fractures. To simulate these virus pathways, a fixed number (1000) of numerical particles were released into the grid cell that simulated the sinkhole, permitting the visualization of all the possible pathways of the injected wastewater in groundwater and those of the viruses released via strong detachment after a flood event. Particles entering a channel intersection (i.e., the generic block centered grid node) were distributed into the outlet branches following the density of probability function f(**x**) values, where **x** is the vector of the spatial particle position (Masciopinto et al., 2010). Dagan (1989, p. 271–283) introduced the Taylor expansion of f(**x**) to explain the vector displacement of a virus particle.

In this study a Gaussian probability distribution conditioned by higher water velocities outflowing from a generic grid node was used. This means that the majority of inflowing particles entering an intersection (node) preferentially flowed out in a sequence of channels (i.e., pathways) with higher velocities. Fig. 3 shows the preferential flow pathways in groundwater from the sinkhole (violet star) where runoff from flooding was injected in the study area (12 × 13 km^2). The green triangles and cyan areas respectively show the soil spreading (or irrigation) sites and the artificial recharge ditches that are currently recharging groundwater with treated municipal effluents. The yellow areas (i.e. sectors), oriented on the basis of groundwater velocity direction, represent subsoil where strong detachment of viruses previously loaded by recharge operations could potentially occur, i.e., where *terra rossa* came into contact with floodwater flowing through fractures with low ionic strength (IS) (4.3 mM), leading to virus detachment.

An IS of 23–25 mM was estimated in the summer period for groundwater unaffected by floodwater runoff, since electrolyte concentrations are expected to be highest during this season (Table 3). The transport model accounted for the perturbation of the chemical qualities of the flowing groundwater, i.e., organic compounds, electrolyte concentrations, IS, temperature, and *p*H (Bradford et al., 2012; Pedley et al., 2006; p. 66; Yates and Jury, 1995), resulting from flood runoff injection that has affected either virus attachment/detachment or inactivation. Indeed, the perturbation in IS of water flowing through fractures could lead to soil surface chemistry and environmental conditions that are less favorable for virus attachment to *terra rossa* sediments because of increased repulsive double layer forces between the negatively charged surfaces of both viruses and *terra rossa* minerals. Experimental evidence for the influence of perturbations in IS on virus detachment (up to twice the injected virus concentration in perturbed flow) from *terra rossa* in water flowing in fractures was provided by Masciopinto and Visino (2017).

The detached viruses would follow the same groundwater pathways of the virus injected with wastewater runoff into the sinkhole. The total concentration of virus particles, resulting from continuous runoff injection, collected at the target well was defined as follows:

$$C_T[\boldsymbol{x}(t)] = \frac{\sum_{k=1}^{nc} \Delta m_k [f(\mathbf{x}_k)]}{W_{0_r}} C_{0_r} e^{-\overline{\lambda}\tau_k} \quad (2)$$

where Δm_k[f(**x**)] is the expected mass of viruses transported by a generic cluster (*k*) of particles with travel time τ_k, i.e., it is the fraction of the total mass W_{0r} of injected viruses (1000) by runoff in groundwater; and *nc* is the number of clusters with different travel times τ_k of the collected particles at the target well.

The maximum target concentration for the detachment of a large amount of previously accumulated viruses in the groundwater, over several months of recharge and/or irrigation with reclaimed water, was then determined by considering the pulse of virus injection at the detachment position (Fig. 4):

$$C_T[\boldsymbol{x}(t)] = \frac{\Delta m_k}{W_{0_d}} C_{0d} f(\boldsymbol{x}_k) e^{-\overline{\lambda}\tau_k} \quad (2a)$$

where $\Delta m_k f(\boldsymbol{x}_k)$ is the expected mass of transported viruses by cluster *k* of particles with travel time τ_k, which is the modal time, i.e., travel time of most particles to reach the target well from the detachment position; and C_{0d} is the concentration of amount (mass) of instantaneously detached/re-suspended viruses into fracture flow represented by total particle injected (1000).

In both Eqs. (2) and (2a), $\overline{\lambda}$ (t^{-1}) accounts for the time-dependent virus reduction rate (Masciopinto et al., 2011) resulting from the attachment, inactivation, filtration, detachment, or re-attachment of viruses during their transport in fractures. The equation for $\overline{\lambda}$ was derived by the analytical solution of suspended virus transport in two-dimensional fractures by application of the Lagrange theoretical approach (see Appendix A). Furthermore, $\overline{\lambda}$ is a function of the average fracture aperture, virus attachment/detachment coefficients, suspended and attached inactivation rates, and travel time τ of viruses in groundwater, because the reduced capacity of detached viruses to reattach is time-dependent.

Fig. 4 shows the conceptual representation of the boundary/initial conditions applied to solve Eqs. (2) and (2a) that simulated the indirect contamination of well I1147 during summer 2017 due to flood runoff injection in October 2016. In fact, virus occurrence in groundwater was more likely in summer. The following least conservative assumptions were made: 1) a maximum distance of 2 km of the virus detachment area from the pumping well was chosen, 2) only one source of virus detachment was considered, and 3) the detached concentration C_0d of viruses was fixed at 9.24 IP/ml, i.e., 45% of the average counts of somatic coliphages (20.6 cfu/ml) that were measured in the Salento groundwater at the Nardò injection site (sinkhole) during flooding in 2006/2007 (Masciopinto et al., 2011). Similar boundary/initial conditions were assumed for flooding during November 2015, which could have indirectly contaminated well I1126 during summer 2017. Moreover, the interaction between flooding in 2015 and 2016 (Supermeteo, 2018) was neglected.

The upper limit for the survival time of viruses in fractures has been estimated as 15 months (460 days) after injection time (Borchardt et al., 2007; Nevecherya et al., 2005). The time-dependent reduction rate $\overline{\lambda}$ of viruses in fractures was calculated as $0.0496 \pm 4 \cdot 10^{-3}$ day^{-1}, whereas the inactivation rate for both attached and suspended viruses was fixed at 0.036 day^{-1} (John and Rose, 2005), as estimated by Yates et al. (1985) for PV 1 in well water at 12–13 °C. Following particle tracking model solutions, the predicted C_T was thus estimated at 1.0 ± 0.23 and 0.6 ± 0.14 IP/l in wells I1147 and I1126, respectively, and the virus runoff contribution to the contamination of these wells was negligible ($<2.7 \pm 0.6 \cdot 10^{-4}$ IP/l).

4.3. Quantitative health-risk estimation

A detailed study of the population that might be exposed to pathogens through the ingestion of drinking water was carried out by considering both community and private wells that supply towns, farms, tourist villages, and country houses. The coastline of the Salento peninsula borders the Adriatic Sea and has many pleasant beaches (e.g., Torre dell'Orso, Laghi Alimini, S. Andrea, Otranto, and Porto Badisco) that are intensively populated each summer. Consequently, both residential and tourist populations have been included in the risk impact calculations.

4.4. Exposure assessment

The risk assessment was carried out by assuming a daily drinking-water intake of 1.0 l per person. This was in the 50th percentile of the collected dataset and is currently the most probable (50%) daily

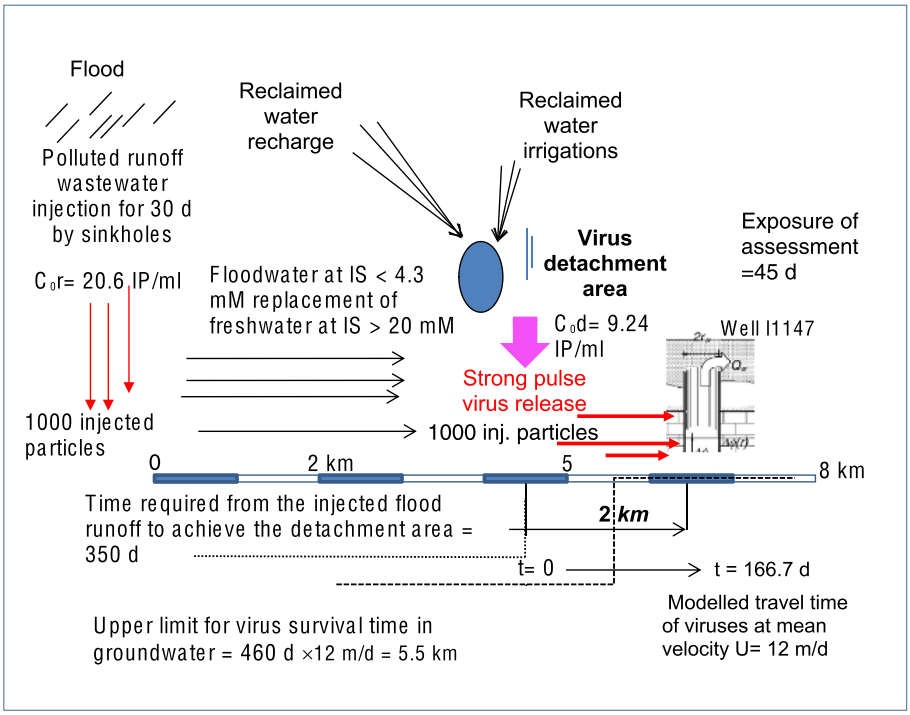

Fig. 4. Least conservative conditions assumed for virus transport modeling in fractures for simulating the indirect contamination of well I1147 by strong detachment of previously accumulated viruses in groundwater during several months of recharge and irrigation with reclaimed water.

drinking water intake for the population of Salento (www.istat.it). The individual probability of infection was estimated using a β-Poisson dose-response model (Crockett et al., 1996; Crabtree et al., 1997) based on the assumption that the infective viruses were randomly (according to a Poisson distribution) monodispersed (i.e., non-aggregated) (Gerba and Betancourt, 2017) in the dose (Haas et al., 2014; Haas, 1996; Furumoto and Mickey, 1967):

$$P_{i,v} \cong 1 - \left(1 + \frac{ID}{\beta}\right)^{-\alpha} \tag{3}$$

The model also assumes a binomial (beta) distribution of the probability of virus-host survival to initiate the infection and that the minimum number of surviving viruses is one. *ID* is the infectious dose (i.e., count) of virus particles (IP) in the daily volume of drinking water intake; α (−), e.g., the slope of the probability of infection vs ID curve and β (IP), is a dose related to the median value (ID_{50}) that has a 50% probability (Haas et al., 2014) of infecting the host who ingested the considered IPs (Table 4). In this study, the maximum C_T of water from well I1147 was considered in the exposure assessment.

This was further reduced to 33% of the predicted model concentration to account for the chlorination barrier efficacy (Masciopinto et al., 2007), i.e., $ID = 1.0\ \text{IP/l} \times 0.33 \times 1\ \text{l} = 0.33$ IP. Table 5 further shows the proposed Echo-11 coefficients: β was set to be equal to the minimum infection dose (MID) (Yezli and Otter, 2011), and α was derived from the known relationships between α, β, and ID_{50} given by Haas et al. (2014) for the approximate β-Poisson solution in Eq. (3), when β and ID_{50} are known.

The exponential approximation of the model in Eq. (3) was derived by assuming that each ingested virus has an identical probability of infection (Haas et al., 2014):

$$P_{i,v} = 1 - \exp\left(-\frac{ID}{\beta_1}\right) \tag{4}$$

where β_1 is the virus count related to the median dose (Masago et al., 2006) of the 50% probability of infection. The proposed β_1 for PV 1/SM was derived by selecting a value close to ID_{50} (2–3 IP). Fig. 5 shows a comparison between the daily probabilities of infections of the considered enteric viruses given by Eqs. (3) and (4) for infective doses of <10 IP. In addition, since the contaminated drinking water may have simultaneously contained HAV, AdV, NoV, RoV, and EV, the cumulative (all viruses) daily probability of infection (see Fig. 5) was calculated as (de Man et al., 2014; Haas, 1996)

$$P_{Daily} = 1 - \prod_{i}^{nv} (1 - P_{i,v}) \tag{5}$$

where $P_{i,v}$ is the daily probability of infection of the specific virus considered; and *nv* is the total number of viruses considered (five in this study). The final calculation required estimations of probabilities of occurrence (PO) for each virus, i.e., PO_{HAV}, PO_{AdV}, PO_{NoV}, PO_{RoV}, and PO_{EV}, with the condition of $\Sigma\ ID_v = ID$. In this study, the infectious dose for each virus (Table 6), once ingested, was estimated by partitioning the target concentration into sub concentrations proportional to MID. Subsequently, the annual (and seasonal) probability of infection was calculated (de Man et al., 2014):

$$P_{Y,v} = 1 - (1 - P_{i,v})^{ep} \tag{6}$$

where the exposure period *ep*, was reduced from 365 to 45 days per year when only summer was considered.

The cumulative annual probability of infection (P_Y) was determined as follows:

$$P_Y = 1 - \prod_{i}^{nv} (1 - P_{Y,v}) \tag{7}$$

or

$$P_Y = 1 - (1 - P_{Daily})^{ep} \tag{8}$$

The measured cumulative risk for viral diseases in the study area was estimated by multiplying P_Y by the exposed population, considering

Table 4
Coefficients of dose-response probability of infection applied in this study per 1 ml of contaminated drinking water intake.

	Dose-response model	Model coefficients	References
HAV	Exponential (β_1)	1.8229 IP	Haas and Eisenberg, 2001
RoV	Approximate β-Poisson (α and β)	0.253 and 0.422 IP	Teunis and Havelaar, 2010
AdV	Exponential (β_1)	2.397 IP	Crabtree et al., 1997
NoV	Exact β-Poisson (α and β)[a]	0.04 and 0.055 IP	Teunis et al., 2008
	Exponential (β_1)	2.375 IP = 0.05 / (0.04 + 0.055)	Sokolova et al., 2015
EV			
Echo-12	Approximate β-Poisson (α and β)	0.401 and 227.2 IP	Teunis et al., 1996
Echo-11	Approximate β-Poisson (α and β)	0.4021 and 17 IP	This work
	Exponential (β_1)	78.3 IP	Mc Bride et al., 2013; Haas and Eisenberg, 2001
PV1/SM	Exponential (β_1)	2.8182 IP	This work

[a] β and β_1 are for 0.1 g or 0.1 ml of contaminated drinking water intake.

both primary and secondary morbidity factors M_p and M_s (Eisenberg et al., 2004).

The risk model in this study introduced a new antimicrobial resistance morbidity coefficient M_{AR} (1.5%) to account for additional (secondary) infections due to failures in clinical treatments. During the calibration of the risk impact (Fig. 6), host susceptibility (1 - immunity) was selected as a constant value based on the findings of previous studies (Masciopinto et al., 2007; Lopalco et al., 2001), as was the percentage of underreported and asymptomatic HAV cases (ECDC, 2018). The bounds of uncertainty were also reported throughout each subpopulation in terms of age groups (Fig. 6).

In this calibration step, the annual probability of a hepatitis A infection (Fig. 6) was estimated using Eq. (6) for the subpopulation data of Lecce province collected by the Italian National Institute of Statistics during 2016 (www.istat.it). The HAV diseases collected in 2017 were not considered in this study due to anomalous increases in confirmed HAV infections across Europe and in Salento (see Fig. 1) during this year. The uncertainty in the C_T model predictions was included in the risk calculations by providing a probability interval of the estimated number of diseases. Comparing the model predictions with confirmed HAV cases allowed for the calibration of the risk model's primary and secondary morbidity coefficients.

The calibration was performed by fixing drinking water as the primary source of HAV diseases (59% of total confirmed cases). Calculations of the probability of annual HAV disease incidence by age group were performed for the entire population of Lecce province by accounting for both the morbidity and susceptibility of the population. The same risk model was then applied to a subpopulation of the Salento area that may currently be exposed to the simultaneous ingestion of AdV, NoV, HAV, RoV, and EV (i.e., PV 1/SM and Echo-11) via drinking water. This risk calculation was then applied to resident and tourist populations of the neighboring coastal area Otranto recorded during 2017 (Regione Puglia, 2018).

5. Results and discussion

The well monitoring results showed very low concentrations of TBC, total coliforms, and *Escherichia coli*, as well as of nitrates, although some traces of ammonia and *E. coli* at 21 cfu/ml were observed in water sampled during April 2017 from wells I1190 and I1147, respectively. Water samples from wells I1126, I1147 and I1190 tested positive for NoV GII.4 at 4.48 ± 1.07 gc/l, EV, and HAV IB during April 2017. The predicted total number of diseases that could potentially affect both residents and tourists in the study area are shown in Table 6. The median (50%)

Table 5
Probabilities of infections (in bold) and model calibration for disease forecasts. Population data were provided by the Italian National Institute of Statistics (www.istat.it/) and hepatitis A illness data were provided by a regional sanitary surveillance database (ASL, 2018).

	Total	HAV	AdV	NoV	EV	RoV
C_{Tmin} (IP/l)		0.30	1.66	18.00	13.00	1
ID_v (IP)	0.33 ± 0.08	0.003	0.016	0.175	0.126	0.01
$P_{i,v}$		$1.62 \cdot 10^{-6}$	$6.73 \cdot 10^{-6}$	$7.36 \cdot 10^{-5}$	$4.78 \cdot 10^{-5}$	$9.67 \cdot 10^{-6}$
All viruses: P_{Daily}	**$1.39 \pm 0.3 \cdot 10^{-4}$**					
ep (days)	365					
$P_{Y,v}$		$5.91 \cdot 10^{-4}$	$2.53 \cdot 10^{-3}$	$2.54 \cdot 10^{-2}$	$1.66 \cdot 10^{-3}$	$3.88 \cdot 10^{-3}$
ep (days)	45					
$P_{Y,v}$=		$7.29 \cdot 10^{-5}$	$3.03 \cdot 10^{-4}$	$3.31 \cdot 10^{-3}$	$2.15 \cdot 10^{-3}$	$4.35 \cdot 10^{-4}$
All viruses P_Y	**$6.26 \pm 1.44 \cdot 10^{-3}$**	Season				
	$4.77 \pm 1.1 \cdot 10^{-2}$	Year				
Tolerable risk for Rotavirus	$3.1 \cdot 10^{-3}$		(WHO, 2011)			

RISK model calibration (hepatitis A cases)

Years		Age group (years)				
2007–2016	Average	0–14	15–24	25–34	35–54	≥55
Residents	804,239	104,131	84,568	91,406	236,973	287,161
M_P	0.1	0.2	0.15	0.3	0.2	0.03
M_s	0.1					
M_{AR}	0.015					
Immunity	0.17	94	90	80	90	95
Underreported	0.64					
Exp. HAV infections	3.2 ± 0.6	0.3	0.3	1.3	1.1	0.1
Error bars (±) (%)	0.73	0.07	0.07	0.3	0.26	0.02
% to tot notified		5.5	5.6	24.2	20.9	1.9
Not. HAV infections	5.4	0.6	0.7	2.1	1.9	0.1
% of tot notified		11.1	13.0	38.9	35.2	1.9
Δ(expected − notified) (%)		−5.6	−7.4	−14.7	−14.3	0.0

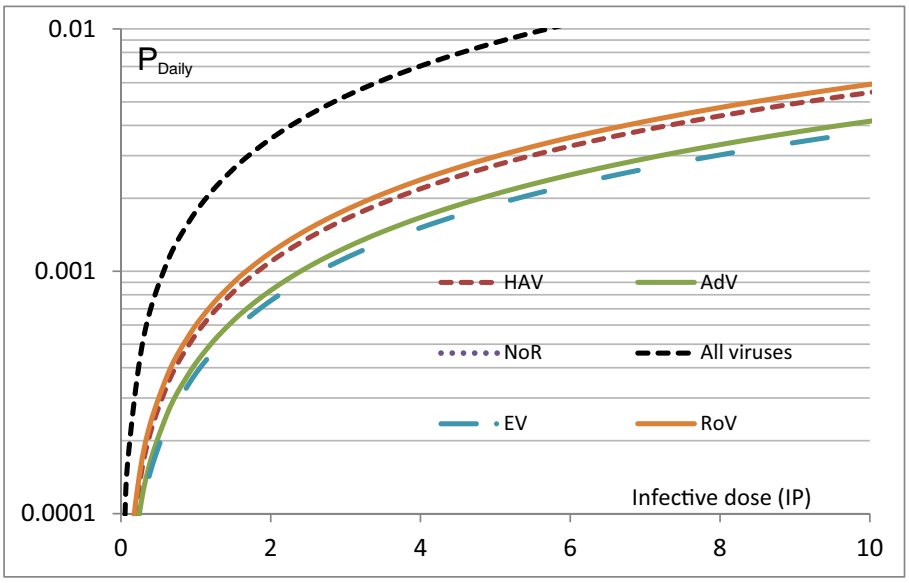

Fig. 5. Individual and cumulative (all viruses) daily probabilities for adenovirus, enterovirus, hepatitis A, rotavirus, and norovirus infections vs infective doses in 1 l of drinking water per day.

Table 6
Predictions of number of diseases (as of 2017) in the Salento coastal area during summer.

Cumulate virus infections prediction							
		HAV	AdV	NoV	EV		RoV
Summer 2017 residents and tourists	1,786,446				Polio 1/SM	ECHO-11	
Immunity (%)		0.88	0.70	0.56	0.98	0.75	0.75
Underreported							
Expected individual virus diseases		2	18	297	4	7	22
Expected cumulative annual diseases	349						
Incidence (×100,000)	19.6 ± 4.5						

seasonal health risk from the diseases for the population of Salento was estimated to be $6.3 \pm 1.4 \cdot 10^{-3}$. This risk impact was roughly twice the tolerable risk ($3.1 \cdot 10^{-3}$) for RoV infections suggested by WHO (2011) guidelines for high-income countries. It should be noted that the most prevalent diseases were NoV (297 cases) and RoV (22 cases), whereas the remaining diseases were attributable to AdV (18 cases), ECHO-11 (7 cases), PV (4 cases), and HAV (2 cases). This may be explained by the relatively high host susceptibility (0.45) applied in the calculations, though higher values (0.6–0.7) are usually applied in NoV dose-response models (van Abel et al., 2017). These disease predictions also accounted for a secondary morbidity due to antimicrobial drug resistance ($M_{AR} = 0.015$).

The low number of PV infection cases was due to low host susceptibility applied (0.02) and the Italian vaccination program. Therefore, PV infections may have only affected unvaccinated individuals. In fact, in Italy, PV vaccination strategies have changed over time, and the oral polio vaccine was replaced by the inactivated vaccine in 2002 (when the eradication of poliomyelitis was achieved in the European region),

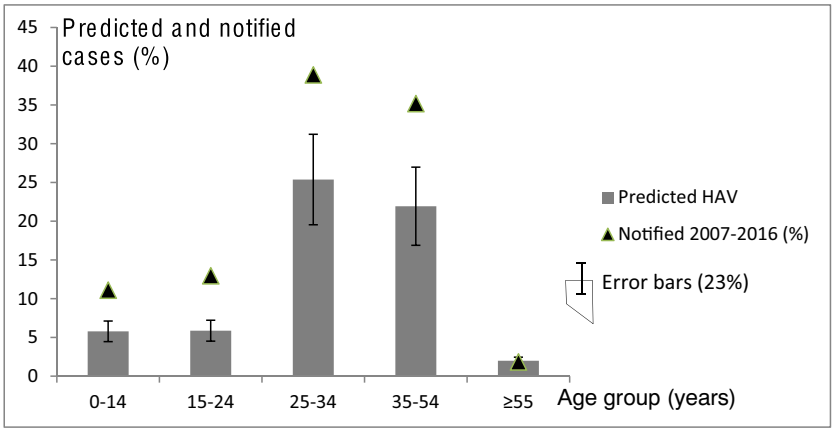

Fig. 6. Calibration of the risk impact of waterborne viral diseases using 59% of the average confirmed hepatitis A cases in Lecce province (Salento, Italy) by age group from 2007 to 2016. The remaining 41% of the hepatitis A cases attributable to foodborne and sexual transmission were not considered by this risk impact estimation.

with the aim of preventing vaccine-associated paralytic poliomyelitis and the emergence of vaccine-derived polioviruses. Since the introduction of inactivated vaccine, no polioviruses have been isolated from suspected acute flaccid paralysis cases, and only a small number of Sabin-like PVs, probably excreted by individuals immunized with oral polio vaccine abroad (poliovirus importation), were isolated in sewage via environmental surveillance, confirming the polio-free status of Italy (Delogu et al., 2018).

Disease incidence was estimated to be 19.6 ± 4.5% per 100,000 individuals. This corresponds to a total disease burden of 4.89 DALYs per season on average, using the conversion factor of $1.4 \cdot 10^{-2}$ of DALYs per case provided by WHO (2011, p. 130) for high-income countries. This disease burden may lead to a significant increase in the annual disease burden per person to $2.74 \pm 0.63 \cdot 10^{-6}$, which is 2.7 times higher than the tolerable burden of $1 \cdot 10^{-6}$ suggested by WHO for RoV infections.

Even though the aim of this study was to show the vulnerability of karst carbonate rocky aquifers to the increasing impact of flooding caused by climate change rather than the estimation of the exact risk assessment value at the test site, the predicted health risk results are valuable for improving management operations and water safety plans in semiarid regions worldwide where groundwater is the main source of drinking water. In fact, our results could easily be adapted for groundwater from different regions, such as the Mediterranean area, Morocco, and Indiana and Wisconsin (USA), where *terra rossa* and carbonate aquifers occur.

At Salento, the chlorination treatment currently applied for water disinfection may yield approximately 4.0 $\log_{10}$ reduction credits. Additional or multi-barrier treatments are nonetheless required to achieve the minimum disinfection performance target of 4.5 $\log_{10}$ credit units that are required to ensure virus removal from drinking water. This estimate was made on the basis of the predicted model concentration of 1.0 ± 0.23 IP/l of water derived from well I1147 by considering the total virus reduction rate coefficient of $0.0496 \pm 4 \cdot 10^{-3}$ day^{-1}. This value was determined (see Appendix A) by means of attached or suspended virus inactivation coefficients of 0.036 day^{-1} and average water velocity of 12 m/day in fractures. This virus reduction rate suggested a negligible runoff contribution to the contamination in well I1147 ($2.7 \pm 0.6 \cdot 10^{-4}$ IP/l) because of long elapsed time from the injection predicted by model, i.e. 350 days (or 11.7 months), which approaches the upper time limit of virus survival in fractured aquifers proposed by other authors, namely 15 months (Borchardt et al., 2007).

The risk of enteric virus infections caused by drinking water ingestion was estimated to be $6.3 \pm 1.4 \cdot 10^{-3}$ in the Salento region, i.e., over twice the tolerable risk for virus infections suggested by WHO ($3.1 \cdot 10^{-3}$). This risk corresponds to a disease burden of 4.89 DALYs per season, i.e. $2.74 \pm 0.63 \cdot 10^{-6}$ per person, which is higher than WHO health outcome target of $1 \cdot 10^{-6}$ and implies a greatly increased annual sanitary cost for the region. The results further suggest that water disinfection treatments to supplement simple chlorination are needed to reduce the disease burden to a tolerable level and achieve the minimum disinfection performance target of 4.5 $\log_{10}$ units of reduction required for drinking water from the Salento aquifer. This estimate was made on the basis of the predicted model concentration of 1.0 virus/l.

Consequently, we strongly recommend monthly monitoring of groundwater in karstified carbonate rock in semiarid regions vulnerable to enteric virus contamination caused by prolonged floodwater injections. Due to the increased height of flooding caused by climate change and hazardous consequences due to possible virus detachment in groundwater, the periodic control of enteric virus occurrence in water from wells of vulnerable aquifers should be imposed by framework directives for drinking water, e.g., those that are currently under revision (http://ec.europa.eu/environment/water/water-drink/review_en.html). Flooding has become more prevalent in European aquifers, and the fecal indicators proposed by Directive 2000/60/EC were insufficient to predict virus fecal contamination of drinking water from wells in the study area.

The quantification of the health impacts of flooding injection and strong virus detachment by means of risk assessment in this study could easily be achieved in many karstic carbonate aquifers in the Mediterranean area, Morocco, and Indiana and Wisconsin (USA), where virus detachment from *terra rossa* can affect drinking water quality. In vulnerable aquifers, water quality monitoring has strategic importance for the protection of water reservoirs from microbial pollution. The water sampling in this study has revealed the health and composition of Salento groundwater. Seasonal changes in groundwater quality and particularly of the virus and electrolyte concentrations have shown that groundwater is more vulnerable to microbial contamination during summer. The upper time limit for survival of viruses injected into the Salento fractured carbonate aquifer was about 12 months on the basis of the estimated total virus reduction rate coefficient of $0.0496 \pm 4 \cdot 10^{-3}$ day^{-1}. This coefficient was determined by considering the inactivation coefficients of attached and suspended viruses (0.036 day^{-1}) and average modeled water flow velocity in fractures of 12 m/day. The estimated upper time limit for virus survival in Salento approached the time limit (15 months) proposed by other studies in fractured aquifers.

6. Conclusions

Flooding height recorded since 1923 at the Galatina station by *Protezione Civile* has tripled over the last 100 years due to the impact of climate change. We showed that strong virus detachment from *terra rossa* sediments in fractures, as a consequence of prolonged runoff injections into sinkholes driven by flood events, can be considered the main cause of the microbial groundwater pollution by enteric viruses observed in two drinking wells in Salento during April 2017. Strong virus detachment from *terra rossa* in groundwater can be activated at remarkable distances from the runoff injection site because of a perturbation in IS of water flowing in fractures. The perturbed flow permits strong detachments of viruses previously attached below sites where treated municipal effluents are used for irrigation and artificial recharge by changing the water's geochemistry at the point of contact with *terra rossa*. The strong release of viruses allows their migration in groundwater to wells located as far as 8 km from the runoff injection site, up to 22 months after the injection time. Available geochemical data and the mathematical model developed in this study permitted the prediction of virus concentrations at target wells I1147 and I1126 during the summer of 2017, i.e., the same wells that were contaminated by NoV GII.4 at 4.48 ± 1.07 gc/l, EV, and HAV IB during April 2017.

Acknowledgments

This study was supported by the Drink Adria IPA ADRIATIC CBC project (1°str/0004) 2013/2016 supported by the European Commission (FESR funds). Sampling and microbiological analyses of water samples were supported by the Puglia Region project: Integrated approach to the management and protection of water resources 2015/2018: FUTURE IN RESEARCH (code DQ5V1R8).

Appendix A

The Lagrange approach (Dagan, 1989) has often been employed in fractured aquifers to study contaminant transport, since it allows for the simplification of governing equations. For suspended virus transport in water flowing in fractures, the following equation is applicable (Masciopinto et al., 2011):

$$\frac{dC[t,\mathbf{x}(t)]}{dt} = -\frac{2}{2b}\left(\frac{\partial C^*}{\partial t} + \lambda^* C^*\right) - \lambda C \tag{A1}$$

$$\frac{\partial C^*}{\partial t} + \lambda^* C^* = r_f \frac{C}{2b} - r_r C^* \tag{A2}$$

where C (M/L^3) is the concentration of suspended viruses; and C^* (M/L^2) is the concentration of attached viruses on the two fracture walls. These virus concentrations are expressed as the mass of virus count per unit area of the fracture surface. Moreover, r_r (t^{-1}) is the virus detachment rate coefficient; r_f (L^2/t) is the attachment rate coefficient; $2b$ is the local aperture in the bedding plane fracture; and λ (t^{-1}) and λ^* (t^{-1}) are the inactivation coefficients for suspended and attached infectious virus particles, respectively. Eq. (A2) can be substituted into Eq. (A1):

$$\frac{dC[t,\mathbf{x}(t)]}{dt} = -\left[\frac{2}{(2b)^2}r_f + \lambda\right]C + \frac{2}{2b}r_r C^* \tag{A3}$$

C^* can be determined from the analytical solution of Eq. (A2) by applying the initial condition of zero attachment concentration, i.e., $C^*(0, \mathbf{x}(t)) = 0$:

$$C^* = \frac{r_f}{2b}\int_0^t C(u,x,y)\ \exp[-(r_r+\lambda^*)(t-u))]du \tag{A4}$$

where u is a dummy integration variable. Eq. (A4) can be substituted into Eq. (A3):

$$\frac{dC[t,\mathbf{x}(t)]}{dt} = -\left[\frac{2}{(2b)^2}r_f + \lambda\right]C + \frac{2}{(2b)^2}r_r r_f \int_o^t C(u,x,y)\ \exp[-(r_r+\lambda^*)(t-u)]du \tag{A5}$$

Eq. (A5) is a linear first-order differential equation:

$$\frac{dC[t,\mathbf{x}(t)]}{dt}\frac{1}{C[t,\mathbf{x}(t)]} = -A_1 + A_2 \tag{A6}$$

where $A_1(t^{-1})$ is

$$A_1 = \left(\frac{2}{(2b)^2}r_f + \lambda\right); \tag{A7}$$

and coefficient $A_2(t^{-1})$ can be defined by imposing the similarity between Eqs. (A6) and (A5):

$$C[\tau,\mathbf{x}(\tau)]A_2 = \frac{2}{(2b)^2}r_r r_f \int_o^\tau C(u,x,y)\ \exp[-(r_r+\lambda^*)(\tau-u)]du \tag{A8}$$

where time $t = \tau$ is the time required by the majority of virus particles released in groundwater to arrive at the target well. Eq. (A8) can be solved to produce:

$$A_2 = -\frac{2}{(2b)^2}r_r r_f \frac{1}{r_r+\lambda^*}\ \exp[-(r_r+\lambda^*)\tau] \tag{A9}$$

Thus, the coefficient of virus reduction rate in water flowing in fractures can be estimated from Eq. (A6):

$$\overline{\lambda} = (A_1 - A_2) \tag{A10}$$

It should be noted that $\overline{\lambda}$ is the time-dependent coefficient rate of virus reduction in flowing water, since A_2 slightly decreases when time (τ) increases. By substituting Eq. (A10) into Eq. (A6), the exponential solutions in Eqs. (2) and (2a) were obtained. The values of specific coefficients applied at Salento (Masciopinto et al., 2011) were as follows:

$2b = 1.3$ mm average fracture aperture
$U = 12$ m/day mean flow velocity $= \sqrt{(U_x^2 + U_y^2)}$
$k = 3.2 \cdot 10^{-8}$ m
virus deposition coefficient
$F_c = 0.03$ dynamic block function value
$r_r = 3.425 \cdot 10^{-4}$ day^{-1}
virus detachment coefficient
$r_f = 1.15 \cdot 10^{-8}$ m^2/day
virus attachment coefficient $= k \cdot U \cdot F_c$
$\lambda = \lambda^* = 0.036$ day^{-1}
virus inactivation coefficients.

References

ASL, Local Sanitary Facility, 2018. Numero di casi notificati di epatite A, per anno e classe d'età: anni 2007–2017 (Notified Cases of Hepatitis A per Year by Age Group: 2007–2017 Years. Regional Database on Infective Illnesses). Archivio regionale Sistema Informativo Malattie Infettive, Lecce (in Italian).

Ayuso-Gabella, N., Page, D., Masciopinto, C., Aharoni, A., Salgot, M., Wintgens, T., 2011. Quantifying the effect of Managed Aquifer Recharge on the microbiological human health risks of irrigating crops with recycled water. Agric. Water Manag. https://doi.org/10.1016/j.agwat.2011.07.014.

Borchardt, M.A., Bradbury, K.R., Gotkowitz, M.B., Cherry, J.A., Parker, B.L., 2007. Human enteric viruses in groundwater from a confined bedrock aquifer. Environ. Sci. Technol. 41 (18), 6606–6612. https://doi.org/10.1021/es071110.

Bradford, S.A., Torkzaban, S., Kim, H., Simunek, J., 2012. Modeling colloid and microorganism transport and release with transients in solution ionic strength. Water Resour. Res. 48 (9), W09509. https://doi.org/10.1029/2012WR012468.

Costafreda, M.I., Bosch, A., Pintó, R.M., 2006. Development, evaluation, and standardization of a realtime TaqMan reverse transcription-PCR assay for quantification of hepatitis A virus in clinical and shellfish samples. Appl. Environ. Microbiol. 72, 3846–3855.

Costán-Longares, A., Montemayor, M., Payán, A., Méndez, J., Jofre, J., Mujeriego, R., Lucena, F., 2018. Microbial indicators and pathogens: removal, relationships and predictive capabilities in water reclamation facilities. Water Res. 42, 4439–4448. https://doi.org/10.1016/j.watres.2008.07.037.

Cotecchia, V., 1977. Studi e ricerche sulle acque sotterranee e sulla intrusione marina in Puglia (Penisola salentina). Quad. IRSA vol. 20. CNR, Rome, pp. 1–462.

Crabtree, K.D., Gerba, C.P., Rose, J.B., Rose, J.B., 1997. Waterborne adenovirus: a risk assessment. Water Sci. Technol. 35 (11–12), 1–6.

Craun, G.F., Calderon, R., 1997. Microbial risk in groundwater systems: epidemiology of waterborne outbreaks. Proc. 12th Annual Symposium, Under the Microscope: Examining Microbes in Groundwater, September 5–6, 1996. American Water Work Association Research Foundation, Boston (MA) Available on line at: https://books.google.it/books.

Crockett, C.S., Haas, C.N., Fazil, A., Rose, J.B., Gerba, G.P., 1996. Prevalence of shigellosis in the U.S.: consistency with dose-response information. Int. J. Food Microbiol. 30, 87–89.

Dagan, G., 1989. Flow and Transport in Porous Formations. Springer-Verlag, New York.

De Giglio, O., Barbuti, G., Trerotoli, P., Brigida, S., Calabrese, A., Di Vittorio, G., Lovero, G., Caggiano, G., Uricchio, V.F., Montagna, M.T., 2016. Microbiological and hydrogeological assessment of groundwater in southern Italy. Environ. Monit. Assess. 188, 638. https://doi.org/10.1007/s10661-016-5655-y.

De Giglio, O., Caggiano, G., Bagordo, F., Barbuti, G., Brigida, S., Lugoli, F., Grassi, T., La Rosa, G., Lucentini, L., Uricchio, V.F., De Donno, A., Montagna, M.T., 2017. Enteric viruses and fecal bacteria indicators to assess groundwater quality and suitability for irrigation. Int. J. Environ. Res. Public Health 14, 558. https://doi.org/10.3390/ijerph14060558.

de Man, H., van den Berg, H.H.J.L., Leenen, E.J.T.M., Schijven, J.F., Schets, F.M., van der Vliet, J.C., van Knapen, F., de Roda Husmana, A.M., 2014. Quantitative assessment of infection risk from exposure to waterborne pathogens in urban floodwater. Water Res. 48, 90–99. https://doi.org/10.1016/j.watres.2013.09.022.

Delogu, R., Battistone, A., Buttinelli, G., et al., 2018. Poliovirus and other enteroviruses from environmental surveillance in Italy, 2009–2015. Food Environ. Virol. https://doi.org/10.1007/s12560-018-9350-8.

Donaldson, K.A., Griffin, D.W., Paul, J.H., 2002. Detection, quantitation and identification of enteroviruses from surface waters and sponge tissue from the Florida Keys using real-time RT-PCR. Water Res. 36, 2505–2514.

ECDC, 2018. Epidemiological update: hepatitis A outbreak in the EU/EEA mostly affecting men who have sex with men. Available at: https://ecdc.europa.eu/en/news-events/epidemiological-update-hepatitis-outbreak-eueea-mostly-affecting-men-who-have-sex-men-0, Accessed date: 2 May 2018.

Eisenberg, J.N.S., Soller, J.A., Scott, J., Eisenberg, D.M., Colford Jr., J.M., 2004. A dynamic model to assess microbial health risks associated with beneficial uses of biosolids. Risk Anal. 24 (1), 221–236.

Fogeda, M., Avellon, A., Cilla, C.G., Echevarria, J.M, 2009. Imported and autochthonous hepatitis E virus strains in Spain. J. Med. Virol. 81, 1743–1749.

Furumoto, W.A., Mickey, R., 1967. A mathematical model for the infectivity-dilution curve of tobacco mosaic virus: theoretical considerations. Virology 32, 216.

Gerba, C.P., Betancourt, W.Q., 2017. Viral aggregation: impact on virus behavior in the environment. Environ. Sci. Technol. 51, 7318–7325. https://doi.org/10.1021/acs.est.6b05835.

Haas, C., 1996. How to average microbial densities to characterize risk. Water Res. 30 (4), 1036–1038.

Haas, J., Eisenberg, J.N.S., 2001. Risk assessment. Chapter 8. In: Fewtrell, L., Bartram, J. (Eds.), Water Quality: Guidelines, Standards & Health. IWA Publishing, London, UK, pp. 161–374.
Haas, C.N., Rose, J.B., Gerba, C.P., 2014. Quantitative Microbial Risk Assessment. second edition. John Wiley & Sons, Inc., Hoboken, New Jersey.
ISO/TS 15216-2, 2013. Microbiology of Food and Animal Feed—Horizontal Method for Determination of Hepatitis A Virus and Norovirus in Food Using Real-time RT-PCR—Part 2: Method for Qualitative Detection. ISO, Geneva, Switzerland.
ISO 15216-1, 2017. International Organization for Standardization Technical Specification. Microbiology of Food and Animal Feed - Horizontal Method for Determination of Hepatitis A Virus and Norovirus in Food Using Real-time RT-PCR - Part 1: Method for Quantification.
John, D., Rose, J.B., 2005. Review of factors affecting microbial survival in groundwater. Environ. Sci. Technol. 39 (19), 7345–7356. https://doi.org/10.1021/es047995w.
Kageyama, T., Kojima, S., Shinohara, M., Uchida, K., Fukushi, S., Hoshino, F.B., et al., 2003. Broadly reactive and highly sensitive assay for Norwalk-like viruses based on real-time quantitative reverse transcription-PCR. J. Clin. Microbiol. 41, 1548–1557.
Keswick, B.H., Gerba, C.P., 1980. Virus in groundwater. Environ. Sci. Technol. 14 (11), 1290–1297. https://doi.org/10.1021/es60171a602.
Kojima, S., Kageyama, T., Fukushi, S., Hoshino, F.B., Shinohara, M., Uchida, K., et al., 2002. Genogroup-specific primers for detection of Norwalk-like viruses. J. Virol. Methods 100, 107–114.
La Rosa, G., Pourshaban, M., Iaconelli, M., Muscillo, M., 2010. Quantitative real-time PCR of enteric viruses in influent and effluent samples from wastewater treatment plants in Italy. Ann. Ist. Super. Sanita 46, 266–273.
La Rosa, G., Della Libera, S., Iaconelli, M., Ciccaglione, A.R., Bruni, R., Taffon, S., Equestre, M., Alfonsi, V., et al., 2014. Surveillance of hepatitis A virus in urban sewages and comparison with cases notified in the course of an outbreak, Italy. BMC Infect. Dis. 14, 419.
La Rosa, G., Sanseverino, I., Della Libera, S., Iaconelli, M., Ferrero, V.E.V., Barra Caracciolo, A., Lettieri, T., 2017. The impact of anthropogenic pressure on the virological quality of water from the Tiber River, Italy. Lett. Appl. Microbiol. 65 (4), 298–305. https://doi.org/10.1111/lam.12774 (Epub 2017 Aug 20).
Loisy, F., Atmar, R.L., Guillon, P., Le Cann, P., Pommepuy, M., Le Guyader, F.S., 2005. Real-time RT-PCR for norovirus screening in shellfish. J. Virol. Methods 123, 1–7.
Lopalco, P.L., Prato, R., Rizzo, C., Germinario, C., Quarto, M., 2001. SIMI and SEIVA: a comparison of two surveillance systems for Hepatitis A in Puglia. BEN - Notiziario ISS 14 (6), 1–4 (June).
Lopalco, P.L., Prato, R., Chironna, M., Germinario, C., Quarto, M., 2008. Control of hepatitis a by universal vaccination of adolescents, Puglia, Italy. Emerg. Infect. Dis. 14 (3), 526–528 (Mar).
Lu, X., Erdman, D.D., 2006. Molecular typing of human adenoviruses by PCR and sequencing of a partial region of the hexon gene. Arch. Virol. 151, 1587–1602.
Lugoli, F., Leopizzi, M.I., Bagordo, F., Grassi, T., Guido, M., De Donno, A., 2011. Widespread microbiological groundwater contamination in the South-eastern Salento (Puglia-Italy). J. Environ. Monit. 13, 192.
Mallinf, 2017. Andamento delle notifiche di malattie infettive prevenibili da vaccino Epatite A, Epatite B, Meningite meningococcica, Morbillo, Parotite, Pertosse, Rosolia, Varicella Puglia, anni 1996–2015 (Bulletin of infectious diseases. Notified cases of infections and temporal trends for years from 1996 to 2015, for population subjected to the vaccination programs started during 1997). Available at: https://www.sanita.puglia.it/web/oer/malattie-infettive, Accessed date: 26 March 2018 (in Italian).
Mallinf, 2018. Bollettino regionale delle malattie infettive. Notifiche di malattie di classe II nel periodo 2001–2016: distribuzione per anno di notifica, Regione Puglia (Bulletin of infectious diseases. Notified cases of diseases of class II during 2001–2016: trends per years on the notified cases). Available at: https://www.vaccinarsinpuglia.org/assets/uploads/files/21/bollettino_malattie_infettive_2001_2016.pdf, Accessed date: 11 May 2018 (in Italian).
Masago, Y., Katayama, H., Watanabe, T., Haramoto, E., Hashimoto, A., Omura, T., Hirata, T., Ohgaki, S., 2006. Quantitative risk assessment of noroviruses in drinking water based on qualitative data in Japan. Environ. Sci. Technol. 40, 7428–7433. https://doi.org/10.1021/es060348f.
Masciopinto, C., 2005. Pumping-well data for conditioning the realization of the fracture aperture field in groundwater flow models. J. Hydrol. 309 (1–4), 210–228. https://doi.org/10.1016/j.jhydrol.2004.12.002.
Masciopinto, C., 2007. Biodegradation of wastewater nitrogen compounds in fractures: laboratory tests and fields observations. J. Contam. Hydrol. 92 (1–4), 230–254. https://doi.org/10.1016/j.jconhyd.2006.12.003.
Masciopinto, C., Caputo, M.C., 2011. Modeling unsaturated–saturated flow and nickel transport in fractured rocks. Vadose Zone J. 10, 1045–1057. https://doi.org/10.2136/vzj2010.0087.
Masciopinto, C., Liso, S.I., 2016. Assessment of the impact of sea-level rise due to climate change on coastal groundwater discharge. Sci. Total Environ., 672–680 https://doi.org/10.1016/j.scitotenv.2016.06.183.
Masciopinto, C., Visino, F., 2017. Strong release of viruses in fracture flow in response to a perturbation in ionic strength: filtration/retention tests and modeling. Water Res. 126, 240–251. https://doi.org/10.1016/j.watres.2017.09.035.
Masciopinto, C., La Mantia, R., Carducci, A., Casini, B., Calvario, A., Jatta, E., 2007. Unsafe tap water in households supplied from groundwater in the Salento region of southern Italy. J. Water Health 5 (1), 129–148. https://doi.org/10.2166/wh.2006.054.
Masciopinto, C., La Mantia, R., Chrysikopoulos, C.V., 2008. Fate and transport of pathogens in a fractured aquifer in the Salento area, Italy. Water Resour. Res. 44, W01404. https://doi.org/10.1029/2006WR005643.
Masciopinto, C., Volpe, A., Palmiotta, D., Cherubini, C., 2010. A combined PHREEQC-2/parallel fracture model for the simulation of laminar/non-laminar flow and contaminant transport with reactions. J. Contam. Hydrol. 117, 94–108. https://doi.org/10.1016/j.jconhyd.2010.07.003.
Masciopinto, C., La Mantia, T., Tandoi, V., Levantesi, C., Divizia, M., Donia, D., Gabrieli, R., Petrinca, A., 2011. Analytical solution for the modeling of the natural time-dependent reduction of waterborne viruses injected into fractured aquifers. Environ. Sci. Technol. 45, 636–642. https://doi.org/10.1021/es102412z.
Masciopinto, C., Vurro, M., Palmisano, V.N., Liso, E.S., 2017. A suitable tool for sustainable groundwater management. Water Resour. Manag. https://doi.org/10.1007/s11269-017-1736-0.
Mc Bride, G.B., Stott, R., Miller, W., Bambic, D., Wuertz, S., 2013. Discharge-based QMRA for estimation of public health risks from exposure to storm waterborne pathogens in recreational waters in the United States. Water Res. 47, 5282–5297.
Merino, E., Banerjee, A., 2008. Terra rossa genesis, implications for karst, and eolian dust: a geodynamic thread. J. Geol. 116, 62–75.
Nevecherya, I.K., Shestakov, V.M., Mazaev, V.T., Shlepnina, T.G., 2005. Survival rate of pathogenic bacteria and viruses. Groundw. Water Resour. 32 (2), 209–214 (Translated from Vodnye Resursy, 32(2), 2005, 232–237).
Paterson, D.L., Wright, H., Harris, P.N.A., 2018. Health risks of flood disasters. Clin. Infect. Dis. 67, 1450–1454. https://doi.org/10.1093/cid/ciy227 (1 November).
Pecson, B.M., Triolo, S.C., Olivieri, S., Chen, E.C., Pisarenko, A.N., Yang, C.-C., Olivieri, A., Haas, C.N., Trussell, R.S., Trussell, R.R., 2017. Reliability of pathogen control in direct potable reuse: performance evaluation and QMRA of a full-scale 1 MGD advanced treatment train. Water Res. 122, 258–268. https://doi.org/10.1016/j.watres.2017.06.014.
Pedley, S., Yates, M., Schijven, J.F., West, J., Howard, G., Barrett, M., 2006. Pathogens: health relevance, transport and attenuation. Chapter 3. In: Schmoll, O., Howard, G., Chilton, J., Chorus, I. (Eds.), Protecting Groundwater for Health: Managing the Quality of Drinking-water Sources. IWA Publishing, London, UK. ISBN: 1843390795.
Peyment, Franco, 1993. Clostridium perfringens and somatic coliphages as indicators of the efficiency of drinking water treatment for virus and protozoan cysts. Appl. Environ. Microbiol. 59 (8), 2418–2424.
Pina, S., Puig, M., Lucena, F., Jofre, J., Girones, R., 1998. Viral pollution in the environment and in shellfish: human adenovirus detection by PCR as an index of human viruses. Appl. Environ. Microbiol. 64, 3376–3382.
Progetto Maggiore, 2015. Servizio di monitoraggio dei corpi idrici sotterranei (Master plan for groundwater quality monitoring in the Puglia region). Off. Bull. Puglia Gov. (37) (in Italian, March 03, 2015).
Regione Puglia, 2018. Report movimento turistico annuale per comune. Dati numerici definitivi, anno 2017. Report: Yearly Movements of Touristic Population per Singe Municipality: Final Data, Year 2017 (in Italian, Bari).
Schoenen, D., 2002. Role of disinfection in suppressing the spread of pathogens with drinking water: possibilities and limitations. Water Res. 36, 3874–3888.
Schultz, A.C., Perelle, S., Di Pasquale, S., Kovac, K., De Medici, D., Fach, P., Sommer, H.M., Hoorfar, J., 2011. Collaborative validation of a rapid method for efficient virus concentration in bottled water. Int. J. Food Microbiol. 145, S158–S166.
SEIEVA, Epidemiological Integrated System for Acute Viral Hepatitis, 2017. Sistema Epidemiologico Integrato delle Epatiti Virali Acute: Aggiornamento epidemiologico a novembre 2017 (Updating of Epidemiological Data Collected, November 2017). Bulletin no. 1-2017 (in Italian).
Sokolova, E., Petterson, S.R., Dienus, O., Nyströmd, F., Lindgren, P.-E., Pettersson, T.J.R., 2015. Microbial risk assessment of drinking water based on hydrodynamic modelling of pathogen concentrations in source water. Sci. Total Environ. 526, 177–186. https://doi.org/10.1016/j.scitotenv.2015.04.040.
Supermeteo, Metererlogical Center of the Protezione Civile at Salento, 2018. Ottobre 2018: caldo anomalo e precipitazioni record. Mai tanta pioggia a Galatina dal 1923!. Available at: https://www.supermeteo.com/ottobre-2018-caldo-anomalo-e-precipitazioni-record/, Accessed date: 6 December 2018 (in Italian).
Teunis, P.F.M., Havelaar, A.H., 2010. The beta Poisson dose-response model is not a single-hit model. Risk Anal. 20 (4), 513–520.
Teunis, P.F.M., van der Heijeden, der Giessen, var, Havelaar, A.H., 1996. The dose-response relation in human volunteers for gastro-intestinal pathogens. Report No. 284550002. National Insitute of Public Health Inspectorate, Ministry of Public Health, Leuwenhoeklaan 9, NL-3720 BA Bilthoven, The Netherland.
Teunis, P.F.M., Moe, C.L., Liu, P., Miller, S.E., Lindesmith, L., Baric, R.S., Le Pendu, J., Calderon, R.L., 2008. Norwalk virus: how infectious is it? J. Med. Virol. 80 (8), 1468–1476.
van Abel, N., Schoen, M.E., Kissel, J.C., Meschke, J.S., 2017. Comparison of risk predicted by multiple norovirus dose–response models and implications for quantitative microbial risk assessment. Risk Anal. 37 (2). https://doi.org/10.1111/risa.12616.
WHO, World Health Organization, 2011. Guidelines for Drinking-water Quality - 4th ed. NLM Classification: WA 675.
Yates, M.V., Jury, W.A., 1995. On the use of virus transport modeling for determining regulatory compliance. J. Environ. Qual. 24, 1051–1055.
Yates, M.V., Gerba, C.P., Kelley, L.M., 1985. Virus persistence in groundwater. Appl. Environ. Microbiol. 49 (4), 778–781.
Yezli, S., Otter, J.A., 2011. Minimum infective dose of the major human respiratory and enteric viruses transmitted through food and the environment. Food Environ. Virol. 3, 1–30. https://doi.org/10.1007/s12560-011-9056-7.
Zeng, S.Q., Halkosalo, A., Salminen, M., Szakal, E.D., Puustinen, L., Vesikari, T., 2008. One-step quantitative RT-PCR for the detection of Rotavirus in acute gastroenteritis. J. Virol. Methods 153 (2), 238–240. https://doi.org/10.1016/j.jviromet.2008.08.004 (Epub 2008 Sep 17).